April 2009

Metabolic variability in seafloor brines revealed by carbon and sulphur dynamics

Samantha B. Joye

Vladimir A. Samarkin

Beth! N. Orcutt

Ian R. MacDonald

Kai-Uwe Hinrichs

See next page for additional authors

nature geoscience

LETTERS

PUBLISHED ONLINE: 6 APRIL 2009 | DOI: 10.1038/NGEO475

Metabolic variability in seafloor brines revealed by carbon and sulphur dynamics

Samantha B. Joye[1]*, Vladimir A. Samarkin[1], Beth! N. Orcutt[1†], Ian R. MacDonald[2], Kai-Uwe Hinrichs[3], Marcus Elvert[3], Andreas P. Teske[4], Karen G. Lloyd[4], Mark A. Lever[4†], Joseph P. Montoya[5] and Christof D. Meile[1]

Brine fluids that upwell from deep, hot reservoirs below the sea bed supply the sea floor with energy-rich substrates and nutrients that are used by diverse microbial ecosystems. Contemporary hypersaline environments formed by brine seeps may provide insights into the metabolism and distribution of microorganisms on the early Earth[1] or on extraterrestrial bodies[2]. Here we use geochemical and genetic analyses to characterize microbial community composition and metabolism in two seafloor brines in the Gulf of Mexico: an active mud volcano and a quiescent brine pool. Both brine environments are anoxic and hypersaline. However, rates of sulphate reduction and acetate production are much higher in the brine pool, whereas the mud volcano supports much higher rates of methane production. We find no evidence of anaerobic oxidation of methane, despite high methane fluxes at both sites. We conclude that the contrasting microbial community compositions and metabolisms are linked to differences in dissolved-organic-matter input from the deep subsurface and different fluid advection rates between the two sites.

Seafloor mud volcanoes are high-flow environments characterized by vigorous discharge of fluidized mud and gas, and sometimes brine and oil, often at elevated temperature (~50 °C; ref. 3). Over time, fluid flow rates decrease, transitioning some mud volcanoes into quiescent brine pools; brine pools can also form through lateral accumulation of brine into seafloor depressions. Seafloor brines exist in the Black, Red and Mediterranean seas[4–6] and the Gulf of Mexico[7,8]. Ecosystems associated with seafloor brines differ remarkably, depending on fluid composition and flow rates.

Detailed insights into microbial activity in two brines from the northern Gulf of Mexico continental slope, a brine pool with a low fluid-flow rate (Brine Pool NR1; refs 3, 8), and a mud volcano with a vigorous fluid-flow (GB425; refs 7, 8) (Fig. 1), were obtained by collecting depth-stratified fluid samples across the seawater–brine interface. Although fluid flux was not quantified directly, visual comparison of mud discharge and gas escape confirmed differences between the two sites[7,8]. The brine pool fluid was dominated by sulphate reduction and acetogenesis, whereas the mud volcano fluid showed sulphate reduction and methanogenesis from both acetate and bicarbonate despite salinities (>60) typically inhibitory of acetoclastic methanogenesis[9]. Differing distributions of sulphate, dissolved hydrogen and individual volatile fatty acids suggested the presence of functionally distinct microbial populations in the two brines, which was confirmed by radiotracer-based rate measurements and microbial community composition data. Gibbs free energies of reaction did not correlate with dominant modes of metabolism, suggesting that other factors, including osmotic stress, trace-metal limitation, variations in the magnitude and timing of fluid flow and/or labile organic carbon inputs, critically shape these unique ecological niches.

Stratified profiles from the overlying sea water to ~200 cm into the brine fluid were collected using a novel sampling device[8]. The chemical composition and salinity of the endmember brine fluids were similar[8]. The sharp salinity transition between hypersaline brine and sea water, and a higher suspended particle load underscored the rapid fluid-flow regime of the mud volcano (Fig. 2a, f). Both brines were anoxic and mildly sulphidic; concentrations of dissolved inorganic carbon were elevated relative to sea water[8]. Microbial abundance was 100 times higher in brines than in the overlying sea water (Fig. 2a, f), showing that brine-derived substrates produce high microbial biomass. The brines were gas charged; the dominant dissolved alkane was methane (94–99.9%) with a stable carbon isotopic composition, $\delta^{13}C$, of −62‰ (see Supplementary Table S1). Thermogenic methane from nearby sites (−48‰; ref. 10) is enriched in ^{13}C, meaning that a substantial portion of brine methane is derived from biological sources.

The brines are formed through halite dissolution and contained no sulphate[8]. Seawater sulphate diffuses into the brine, and concentrations decreased with depth, reflecting a combination of microbial consumption through sulphate reduction (both sites) and upward advection of sulphate-free brine (mud volcano)[8,11] (Fig. 2b, g).

Hydrogen concentrations exceeding 1 μM are atypical in sulphate-containing marine environments and have been observed only at serpentinite-hosted hydrothermal systems[12], transitional sulphate-depleted marine sediments[13] and microbial mats, where hydrogen accumulates under non-steady-state conditions[14]. These brines were characterized by high concentrations of dissolved hydrogen (Fig. 2b, g). The hydrogen profile in the mud volcano brine was fairly uniform (hundreds of nanomolar), reflecting the potential importance of autotrophic acetogenesis and/or hydrogenotrophic methanogenesis[15]. In the brine pool, however, hydrogen concentration increased to micromolar levels between ~25 and 100 cm and remained high (~6 μM) to 180 cm, promoting

[1]Department of Marine Sciences, University of Georgia, Athens, Georgia 30602-3636, USA, [2]Department of Physical and Environmental Sciences, Texas A&M University, Corpus Christi, Texas 78412, USA, [3]Organic Geochemistry Group, MARUM Center for Marine Environmental Sciences & Department of Geosciences, University of Bremen, 28334 Bremen, Germany, [4]Department of Marine Sciences, University of North Carolina, Chapel Hill, North Carolina 27599, USA, [5]School of Biology, Georgia Institute of Technology, Atlanta, Georgia 30332, USA. †Present addresses: University of Southern California, Los Angeles, California 90089, USA (B.N.O.); Center for Geomicrobiology, Biology Institute, Ny Munkegade 1540 DK-0800 Århus C, Denmark (M.A.L.). *e-mail: mjoye@uga.edu.

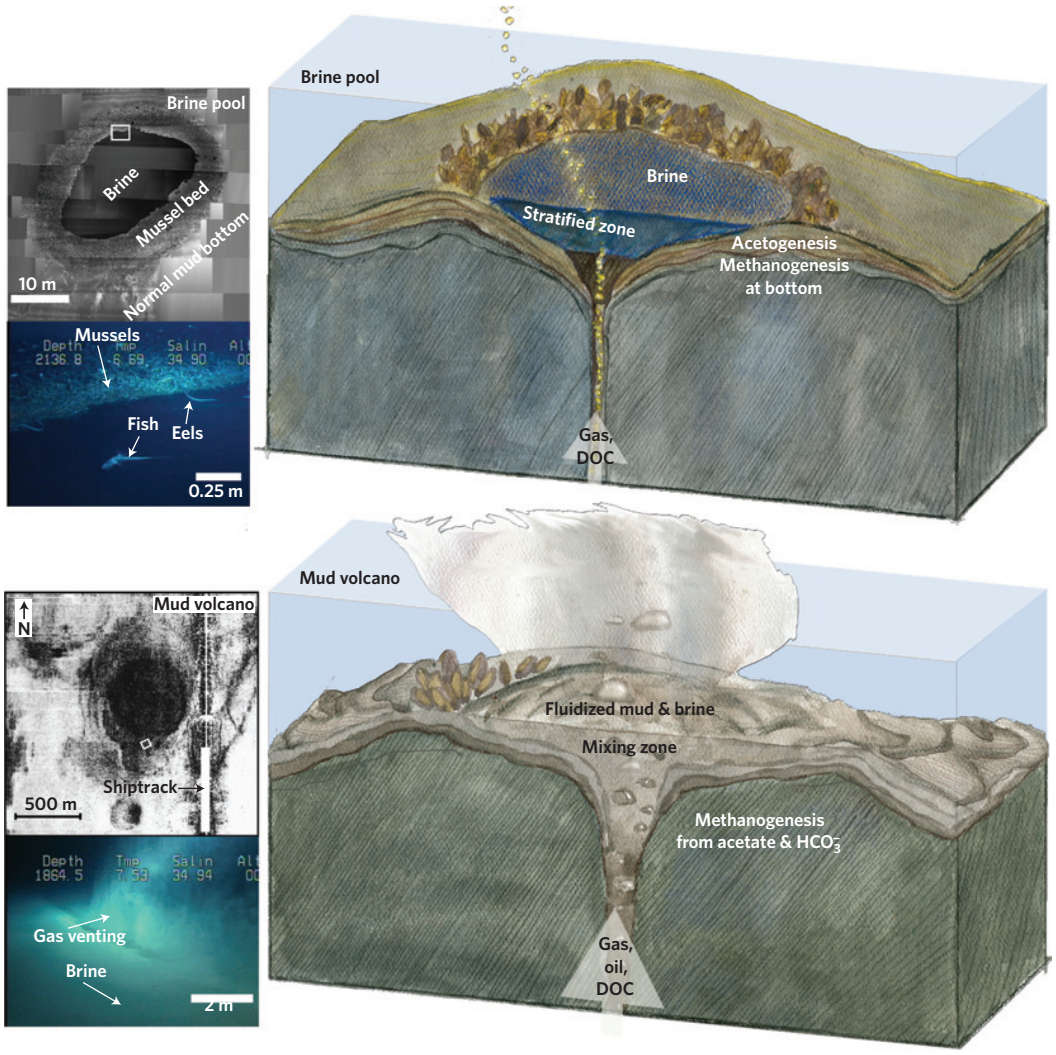

Figure 1 | Schematic diagram illustrating the differences in fluid flow, stratification and surficial chemosynthetic communities between brine pools and mud volcanoes. Brines carry dissolved gases, DOC and oil from the deep subsurface to the sea floor, where these fluids mix with the overlying sea water. The panels to the left show sonar mosaics (upper) and digital photos (lower) of each site (the white square denotes the location of the photograph within the mosaic). Vigorous gas venting from the mud volcano is apparent in the lower panel.

acetogenesis. Such high hydrogen concentrations require active fermentation and substantial inputs of labile organic matter. Concentrations of dissolved organic carbon (DOC) increased with depth (Fig. 2b, g), suggesting a deep-subsurface DOC source. At the brine pool, extra labile DOC from the surrounding chemosynthetic community[7,8] may further stimulate fermentation.

The rates and patterns of microbial activity also differed in the brines, consistent with the observed distributions of sulphate, hydrogen and volatile fatty acids (VFAs). In the brine pool, the most abundant VFA (>70% of the total) was acetate, and low acetate-δ^{13}C values (−30‰) underscored the importance of acetogenesis[16] (Fig. 2c; Supplementary Table S1). Terminal metabolism was dominated by sulphate reduction; methanogenesis rates were orders of magnitude lower. Two comparable peaks of sulphate reduction (60 μmol l^{-1} d^{-1}, hereafter μM d^{-1}) were observed: one in the uppermost sample and one above the brine at 90 cm (Fig. 2d). A deeper zone of sulphate reduction (~20 μM d^{-1}) coincided with increased acetate concentration (Fig. 2c, h; Supplementary Table S1). Acetoclastic methanogenesis rates were generally low (<0.05 nmol l^{-1} d^{-1}, hereafter nM d^{-1}) but increased (0.27 nM d^{-1}) in the deepest sample, where sulphate reduction was absent.

Rates of hydrogenotrophic methanogenesis (Fig. 2d) and of anaerobic oxidation of methane (AOM; data not shown) were below detection (limit ~ 10 pmol l^{-1} d^{-1}) in the brine pool. Whereas the absence of AOM is not surprising (thermodynamic calculations show that methane oxidation is unfavourable), the absence of hydrogenotrophic methanogenesis is perplexing given the abundance of substrates and a large free-energy yield (Fig. 2e). Molecular evidence for the presence of hydrogenotrophic methanogens (see below) suggests this process is either hindered by competition with acetogens or by a metabolic constraint, such as essential trace-metal limitation.

At the mud volcano, sulphate reduction rates were a factor of 10 lower (~5 μM d^{-1}) and were restricted to the overlying sea water and the sulphate-containing mixing zone (Fig. 2i, g). Rates of acetoclastic methanogenesis were two orders of magnitude higher than rates observed at the brine pool (120 versus 0.3 nM d^{-1}) and were 10 times that of hydrogenotrophic methanogenesis (Fig. 2i). Methanogenesis rates increased in the seawater–brine transition zone and were highest within the brine. The similar depth distribution of acetoclastic and hydrogenotrophic methanogenesis indicated contemporaneous activity of both groups of methanogens (Fig. 2i). As in the brine pool, no AOM was detected.

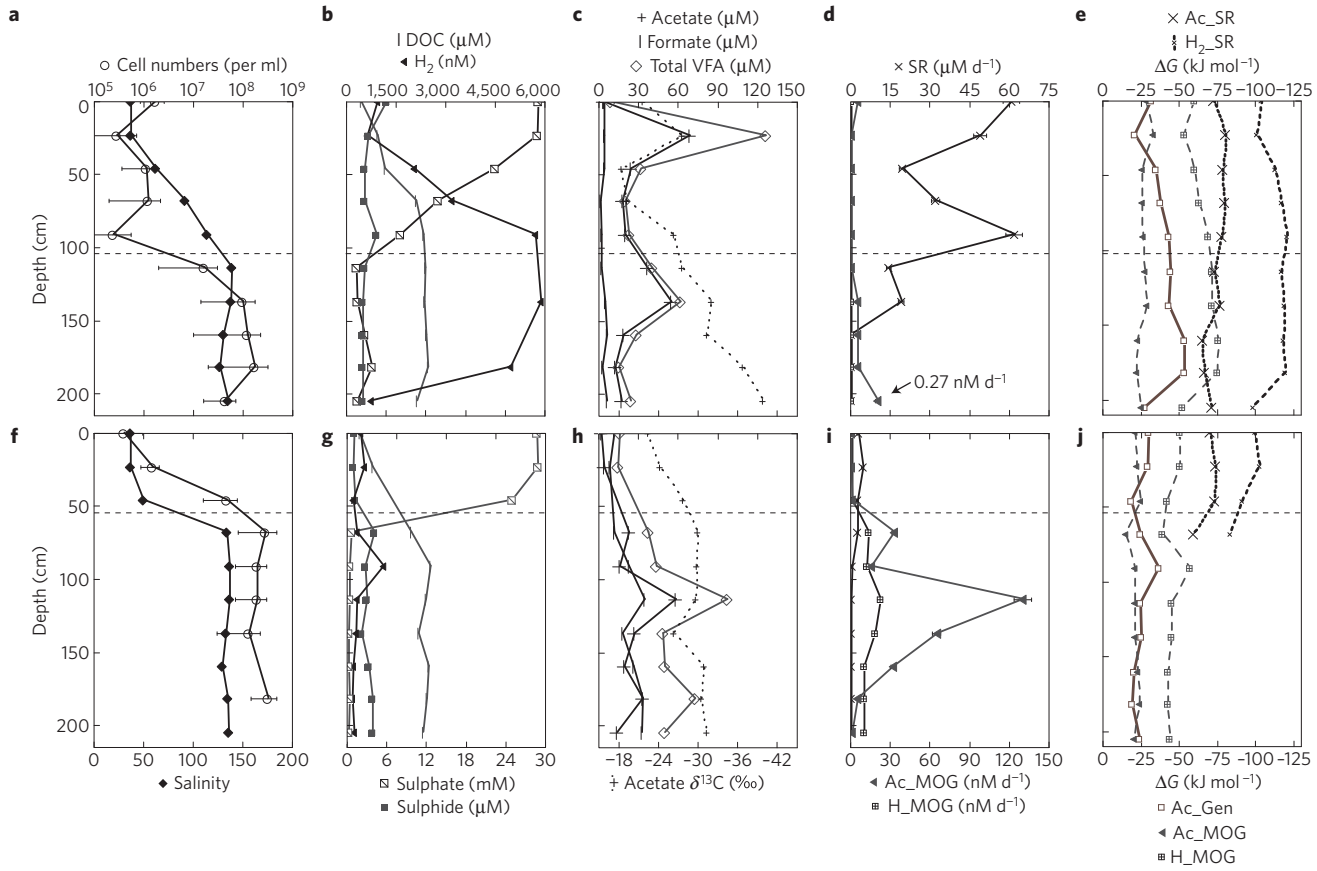

Figure 2 | Depth profiles of microbial abundance, geochemistry, activity and energetics in the brine pool and mud volcano. The horizontal line indicates the pycnocline. **a**–**j**, Microbial abundance and salinity (**a**,**f**); hydrogen (H_2), sulphate (SO_4^{2-}), hydrogen sulphide (H_2S) and DOC concentration (**b**,**g**); VFA concentration and the acetate carbon $\delta^{13}C$ (**c**,**h**); rates of microbial processes (error bars = mean standard deviation; for methanogenesis, the rate scale for **d** is 100 times lower than the scale for **i**) (**d**,**i**); and the Gibbs free energy (ΔG) yield (**e**,**j**) for the brine pool (**a**–**e**) and mud volcano (**f**–**j**). SR: sulphate reduction; Ac_MOG: acetate-based methanogenesis; H_MOG: hydrogen-based methanogenesis; Ac_SR: acetate-based sulphate reduction; H_SR: hydrogen-based sulphate reduction; Ac_Gen: acetatogenesis.

High salinities favour hydrogenotrophic methanogenesis or methanogenesis from non-competitive substrates, such as trimethylamine[9], and known acetoclastic methanogens cannot tolerate high (>60) salinity[9]. This is the first example of acetoclastic methanogenesis at a salinity exceeding 60, suggesting that this pathway may be more important in hypersaline environments than previously assumed.

Free energy yields did not accurately predict the dominant microbial processes (Fig. 2e, j) and illustrated several thermodynamically favourable metabolic pathways. No hydrogenotrophic methanogenesis was detectable in the brine pool, even though the process was energetically favourable. In the mud volcano, hydrogenotrophic methanogenesis occurred at rates lower than those of acetoclastic methanogenesis. The free energy yield of sulphate reduction coupled to acetate oxidation was similar in both brines, yet sulphate reduction rates were 10 times lower in the mud volcano. Owing to the extremely high hydrogen concentrations, methane oxidation to bicarbonate and hydrogen was unfavourable in these brines.

Sequence analysis of 16S ribosomal RNA, dissimilatory sulphite reductase (*dsrAB*) and methyl coenzyeme M reductase (*mcrA*) genes illustrated differences in microbial community composition between the brines (Figs 3 and 4; Supplementary Fig. S1). The uppermost layers of brine pool and mud volcano harboured sulphate-reducing bacterial populations (Desulfosarcinales, *Desulfobacterium*) that oxidize acetate and aromatic compounds (Fig. 3). Related populations within the Desulfobacteraceae were found in the brine pool (but not the mud volcano) by analysis of the *dsrAB* gene (see Supplementary Fig. S2). Propionate-oxidizing sulphate reducers and sulphur-disproportionating bacteria (related to *Desulfobulbus* and *Desulfocapsa*) extend the brine-pool sulphate-reducing bacterial diversity (Fig. 3). In addition, the brine pool contained sulphide- and hydrogen-oxidizing epsilonproteobacteria, consistent with higher hydrogen concentrations (Fig. 3). The presence of sulphate-reducing and sulphide-oxidizing bacteria suggests an active and dynamic sulphur cycle at the brine pool.

The mud volcano contained a lower diversity of sulphate-reducing deltaproteobacterial lineages, with one phylotype each of the Desulfosarcinales and the *Desulfobacterium anilini* group detected (Fig. 3). Non-sulphate-reducing deltaproteobacterial lineages included the Geobacteraceae and Syntrophaceae. Cultured Syntrophaceae representatives are fermentative heterotrophs that grow syntrophically with hydrogen-consuming methanogens, which is consistent with the observed lower hydrogen concentrations and higher rates of hydrogenotrophic methanogenesis at this site.

The *mcrA* sequences retrieved from the mud volcano were most closely related to obligately acetoclastic species (*Methanosaeta sp.*) or those that use methanol or other methylated compounds (*Methanolobus sp.*) (Fig. 4). Surprisingly, *mcrA* gene sequences related to hydrogenotrophic methanogens were not retrieved, suggesting that novel hydrogenotrophs exist at this site or that our sampling was not exhaustive enough to identify them. The *mcrA* gene spectrum matches the dominance of

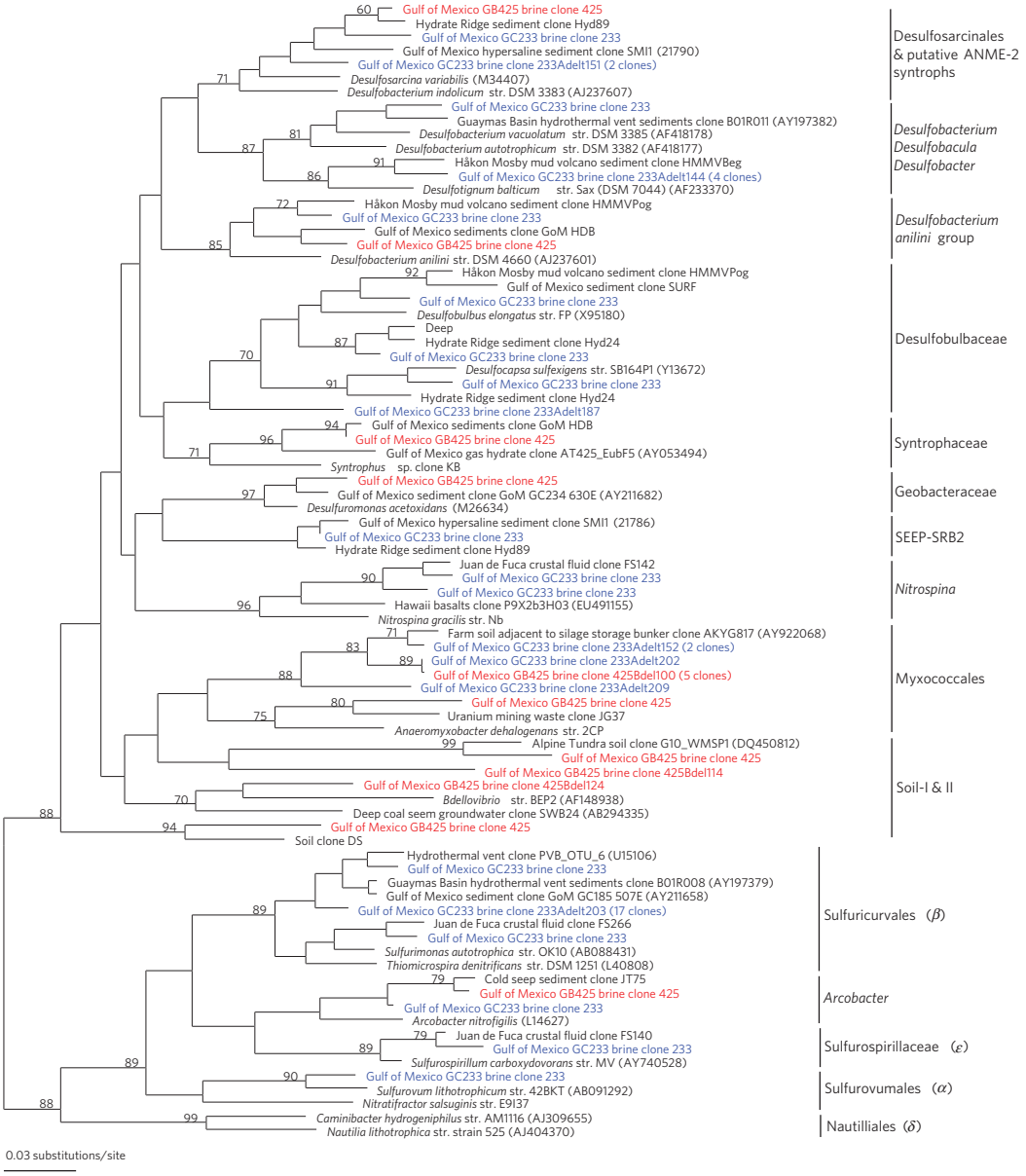

Figure 3 | Phylogeny of deltaproteobacteria and epsilonproteobacteria 16S rRNA from the brine pool (GC233) and the mud volcano (GB425) sites. Blue: brine pool (GC233); red: mud volcano (GB425). The bacterial tree is based on neighbour-joining distances of the 16S rRNA gene; parsimony-based bootstrap values are listed for nodes with greater than 70% support. Environmental clones from different seep sites, vents and geothermal habitats are included to characterize the phylogenetic affinities of the brine pool and mud volcano clones.

acetoclastic over hydrogenotrophic methanogenesis observed in the radiotracer assays (Fig. 2).

The *mcrA* genes recovered from the brine pool fall into four phylogenetic clusters, of which the cultured members include acetoclastic, methylotrophic, hydrogenotrophic and methanotrophic species (Fig. 4): *Methanolobus*-related sequences similar to those detected at the mud volcano; phylotypes similar to subsurface phylotypes from the Peru margin[17] with *Methanosaeta harundinacea* as the closest cultured relative; uncultured Methanomicrobiales that branch with the hydrogenotrophic genera *Methanoculleus* and *Methanospirillum*; and members of the Group e cluster within the Methanosarcinales, with *Methanococcoides burtonii* as the closest relative (Fig. 4). The diverse spectrum of *mcrA* genes in the brine pool is surprising because acetoclastic and hydrogenotrophic methanogenesis rates were extremely low (Fig. 2) and suggests that methanogenesis from alternative substrates, such as methanol or methylated amines, is more important.

Very few results describing rates of microbial activity in seafloor brines exist and none delineates the detailed stratification of microbial processes documented here. Rates of sulphate reduction in these Gulf of Mexico brines were comparable to those in other brines[5,6] (see Supplementary Table S3). Rates of total methanogenesis in Mediterranean brines[5,6] were much higher than the rates of methanogenesis from acetate and hydrogen that we measured (see Supplementary Table S3). The striking difference between microbial activity in these brines and that observed previously in cold-seep sediments[10] is the lack of AOM. High rates of methanogenesis, coupled with the absence of AOM and fluid advection, mean that these brines are potentially significant sources of methane to the overlying water column.

Seafloor brine pools represent dynamic and challenging habitats where microorganisms endure variations in fluid composition and flow regimes, temperature, substrate concentrations, competition with other microbes and high salinity. Acetogenesis was a key

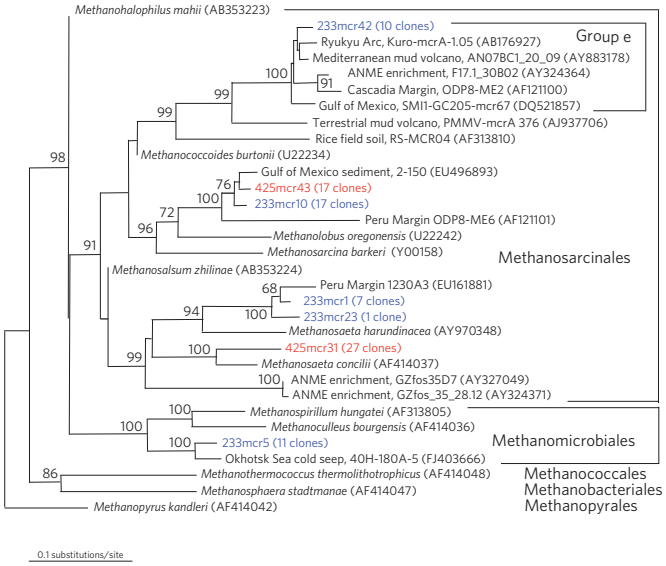

Figure 4 | Neighbour-joining tree of translated *mcrA* sequences with 1,000 repetitions of parsimony-based bootstrap support listed for all nodes with greater than 55%. Blue: brine pool; red: mud volcano.

process in the anaerobic degradation of organic matter in the brine pool, as has been shown in other environments[18]. Fluid flow strongly regulated microbial processes at the Håkon Mosby mud volcano[11], limiting rates of both AOM and sulphate reduction. In Gulf of Mexico brines, sulphate limitation and high hydrogen concentrations probably control sulphate reduction and AOM, respectively. Together with the distinct organic matter sources, the different fluid flow regimes characterizing these Gulf of Mexico brines probably exert selective pressure on the microbial communities, with tighter coupling between oxidative and reductive sulphur reactions observed at the quiescent brine pool. Anaerobic sulphide oxidation could provide a steady sulphate supply to sulphate reducers in the brine pool[8], enabling sulphate reducers to occupy a larger niche. As microbial activity was measurable at the deepest samples collected (Fig. 2d), it is feasible that active microbial assemblages extend deep into the subsurface of the mud volcano systems of the Gulf of Mexico, linking the deep biosphere with ocean bottom habitats.

Methods

Depth-stratified brine samples were collected in 2002 from the brine pool (27°43.4′ N, 92°16.8′ W, water depth 650 m) and the mud volcano (27°33.2′ N, 92°32.4′ W, water depth 600 m) using the RV *Seward Johnson I* and the *Johnson Sea Link* submersible[8]. Concentrations of dissolved hydrocarbons, sulphide, sulphate, VFAs and dissolved hydrogen and radiotracer activity assays were determined as previously described[8,10,19]. Killed controls showed no activity. Brine subsamples were preserved with buffered 3.7% formaldehyde for acridine orange direct counts.

Nucleic acids were extracted from samples as previously described[20]. To compensate for limiting nucleic acid yields, DNA and rRNA were isolated together by omitting the DNAse treatment step. Blank extractions served as negative controls. The epsilonproteobacterial clone 233-Diluted-83G was obtained from a 1:10 nucleic acid extract dilution; all other clones were obtained from undiluted extracts.

Bacterial 16S rRNA/rDNA primers 385f (refs 21 and 22) and 907r (refs 22 and 23) were used for reverse transcription and PCR with the Real Time One Step RNA PCR Kit Ver. 2.0 (Takara). The bacterial 16S rRNA primer 385f is selective, but not specific for deltaproteobacteria, including sulphate-reducing deltaproteobacteria[21,22]; it was used at low stringency to preferentially amplify deltaproteobacteria. Amplification of *dsrAB* and *mcrA* genes required whole genome amplification by multiple strand displacement (RepliG kit, Qiagen), followed by PCR (SpeedStar Taq, Takara) using *dsrAB* primers dsr1f and dsr4r (ref. 24) or *mcrA* primers mcrIRDf and mcrIRDr (ref. 25). For *dsrAB*, nested PCR with primers 1f1 and 1r1 (ref. 26) was necessary to obtain sufficient PCR product for cloning. Details for PCR protocols and primer sequences are provided in Supplementary Information. The samples with the highest radiotracer-measured sulphate reduction rates were tested for *dsrAB* (brine pool surface layer; mud volcano 25 cm depth). The layers of the highest methanogenesis rates were analysed by *mcrA* gene sequencing (brine pool 200 cm; mud volcano 125 cm).

PCR with reverse transcription and nested PCR products were checked by gel electrophoresis on 1.5% agarose gels, purified with the UltraClean PCR Clean-up kit (MoBio) and cloned with the TOPO TA PCR cloning kit (Invitrogen). Plasmid extraction, purification and cycle sequencing for 16S and *dsrAB* were carried out at the Josephine Bay Paul Center (Marine Biological Laboratory); rolling cycle amplification directly from bacterial colonies for *mcrA* was carried out at Genewiz (South Plainfield, New Jersey). Contaminant sequences identified in extraction blanks were subtracted from clone libraries. Sequences were BLAST analysed in GenBank (www.ncbi.nlm.nih.gov/BLAST/), screened for chimaeras with CHECK_CHIMERA (http://rdp8.cme.msu.edu/cgis/chimera.cgi) and aligned and edited in ARB (www.arb-home.de) and SeqPup v0.6 (http://iubio.bio.indiana.edu/soft/molbio/seqpup/java/seqpup-doc.html). Phylogenetic trees were calculated with PAUP4.0* (Sinauer Assoc., Inc) based on maximum likelihood distances corresponding to the General Time Reversible Model. Tree topologies were checked by bootstrap replicas. Primer sequences were excluded from phylogenetic analysis. The sequences have GenBank accession numbers EU334593 to EU334630 and FJ754909 to FJ754998. The *dsrAB* sequences have Genbank accession numbers EU334631 and EU334632. The *mcrA* sequences have Genbank numbers FJ754027 to FJ754033.

For stable carbon isotopic analyses, hydrocarbons were separated on a capillary column and passed through a combustion interface that converted methane to CO_2. Isotopic data were acquired and processed on a ThermoFinnigan Delta Plus XP isotope-ratio-monitoring mass spectrometer using the Isodat NT 2.0 data package. Overall system accuracy was confirmed to be better than 0.5‰ based on a methane standard.

Stable carbon isotopic measurements of acetate were carried out using the Finnigan LC IsoLink interface that couples a ThermoFinnigan Surveyor HPLC to a continuous-flow ThermoFinnigan Delta Plus XP isotope-ratio-monitoring mass spectrometer as described previously[27].

The Gibbs free energy per mole of reaction was estimated for the following metabolic pathways:

Acetogenesis:	$4H_2 + 2HCO_3^- + H^+$
	$\Rightarrow CH_3COO^- + 4H_2O$
Hydrogen-based methanogenesis:	$4H_2 + HCO_3^- + H^+$
	$\Rightarrow CH_4 + 3H_2O$
Hydrogen-based sulphate reduction:	$4H_2 + SO_4^{2-} + H^+$
	$\Rightarrow HS^- + 4H_2O$
Acetate-based methanogenesis:	$CH_3COO^- + H_2O$
	$\Rightarrow CH_4 + HCO_3^-$
Acetate-based sulphate reduction:	$CH_3COO^- + SO_4^{2-}$
	$\Rightarrow HS^- + 2HCO_3^-$
Anaerobic oxidation of methane:	$CH_4 + 3H_2O$
	$\Rightarrow 4H_2 + HCO_3^- + H^+$

Standard-state free energy yields (ΔG^o) were calculated using thermodynamic data from Anderson[28]. Solution densities were estimated as a function of temperature and salinity[29], and activity coefficients of dissolved gases were set to 1. Speciation calculations for solutions of Ca, Mg, Na, K, Fe, Cl, dissolved inorganic carbon, SO_4, NH_4 and acetate at pH 7.5 and 8 °C were carried out with Visual MINTEQ version 2.50, using the specific ion interaction theory activity coefficient model[30]. The free energy yields presented reflect measured dissolved gas concentrations as the radiotracer incubations were carried out at 1 atm.

Received 17 January 2009; accepted 26 February 2009; published online 6 April 2009

References

1. Dundas, I. Was the environment for primordial life hypersaline? *Extremophiles* **2**, 375–377 (1998).
2. Mancinelli, R. L., Fahlen, T. F., Landheim, R. & Klovstad, M. R. Brines and evaporates: Analogs for Martian Life. *Adv. Space Res.* **33**, 1244–1246 (2004).
3. MacDonald, I. R. *et al.* Pulsed oil discharge from a mud volcano. *Geology* **28**, 907–910 (2000).
4. Eder, M. *et al.* Prokaryotic phylogenetic diversity and corresponding geochemical data of the brine-seawater interface of the Shaban Deep. *Environ. Microbiol.* **4**, 758–763 (2002).

5. van der Wielen, P. W. J. J. *et al.* The enigma of prokaryotic life in deep hypersaline anoxic basins. *Science* **307**, 121–123 (2005).
6. Daffonchio, D. *et al.* Stratified prokaryotic network in the oxic–anoxic transition of a deep-sea halocline. *Nature* **440**, 203–207 (2006).
7. MacDonald, I. R. *et al.* Chemosynthetic mussels at a brine-filled pockmark in the northern Gulf of Mexico. *Science* **248**, 1096–1099 (1990).
8. Joye, S. B., MacDonald, I. R., Montoya, J. P. & Peccini, M. Geophysical and geochemical signatures of Gulf of Mexico seafloor brines. *Biogeosciences* **2**, 295–309 (2005).
9. Oren, A. Bioenergetic aspects of halophilism. *Microbiol. Molec. Biol. Rev.* **63**, 334–348 (1999).
10. Orcutt, B. *et al.* Molecular biogeochemistry of sulphate reduction, methanogenesis and the anaerobic oxidation of methane at Gulf of Mexico methane seeps. *Geochim. Cosmochim. Acta* **69**, 4267–4281 (2005).
11. De Beer, D. *et al.* In situ fluxes and zonation of microbial activity in surface sediments of the Haakon Mosby mud volcano. *Limnol. Oceanogr.* **51**, 1315–1331 (2006).
12. Kelley, D. S *et al.* A serpentinite-hosted ecosystem: The lost city hydrothermal field. *Science* **307**, 1428–1434 (2005).
13. Hoehler, T. M., Alperin, M. J., Albert, D. B. & Martens, C. S. Acetogenesis from CO_2 in an anoxic marine sediment. *Limnol. Oceanogr.* **44**, 662–667 (1999).
14. Hoehler, T. M., Bebout, B. M. & Des Marais, D. J. The role of microbial mats in the production of reduced gases on the early Earth. *Nature* **412**, 324–327 (2001).
15. Hoehler, T. M., Alperin, M. J., Albert, D. B. & Martens, C. S. Thermodynamic controls on hydrogen concentrations in anoxic sediments. *Geochim. Cosmochim. Acta* **62**, 1745–1756 (1998).
16. Gelwicks, J. T., Risatti, J. B. & Hayes, J. M. Carbon isotope effects associated with autotrophic acetogenesis. *Org. Geochem.* **14**, 441–446 (1989).
17. Inagaki, F. *et al.* Biogeographical distribution and diversity of microbes in methane-hydrate bearing deep marine sediments on the Pacific Ocean Margin. *Proc. Natl Acad. Sci. USA.* **103**, 2815–2820 (2006).
18. Drake, H. L., Küsel, K. & Matthies, C. in *The Prokaryotes* 3rd edn, Vol. 2 (eds Dworkin, M., Falkow, S., Rosenberg, E., Schleifer, K.-H. & Sttakebrandt, E.) 354–420 (Springer, 2007).
19. Hoehler, T. M., Alperin, M. J., Albert, D. B. & Martens, C. S. Field and laboratory studies of methane oxidation in anoxic marine sediment—evidence for a methanogen-sulfate reducer consortium. *Glob. Biogeochem. Cycles* **8**, 451–463 (1994).
20. Biddle, J.F. *et al.* Heterotrophic archaea dominate sedimentary subsurface ecosystems off Peru. *Proc. Natl Acad. Sci. USA* **103**, 3846–3851 (2006).
21. Amann, R. I. *et al.* Molecular and microscopic identification of sulfate-reducing bacteria in multispecies biofilms. *Appl. Environ. Microbiol.* **58**, 614–623 (1992).
22. Teske, A. *et al.* Sulfate-reducing bacteria and their activities in cyanobacterial mats of Solar Lake (Sinai, Egypt). *Appl. Environ. Microbiol.* **64**, 2943–2951 (1998).
23. Muyzer, G. *et al.* Phylogenetic relationships of *Thiomicrospira* species and their identification in deep-sea hydrothermal vent samples by denaturing gradient gel electrophoresis of 16S rDNA fragments. *Arch. Microbiol.* **164**, 165–172 (1995).
24. Wagner, M. *et al.* Phylogeny of dissimilatory sulfite reductases supports an early origin of sulfate respiration. *J. Bacteriol.* **180**, 2975–2982 (1998).
25. Lever, M. A. *Anaerobic Carbon Cycling Pathways in the Deep Subseafloor Investigated via Functional Genes, Chemical Gradients, Stable Carbon Isotopes, and Thermodynamic Calculations.* PhD Dissertation, Univ. North Carolina at Chapel Hill (2008).
26. Dhillon, A. *et al.* Molecular characterization of sulfate-reducing bacteria in the Guaymas Basin. *Appl. Environ. Microbiol.* **69**, 2765–2772 (2003).
27. Heuer, V. *et al.* Online $\delta^{13}C$ analysis of volatile fatty acids in sediment/porewater systems by liquid chromatography-isotope ratio-mass spectrometry. *Limnol. Oceanogr. Meth.* **4**, 346–357 (2006).
28. Anderson, G. M. *Thermodynamics of Natural Systems* 648 (Cambridge Univ. Press, 2005).
29. McCutcheon, S. C., Martin, J. L. & Barnwell, T. O. in *Handbook of Hydrology* (ed. Maidment, D. R.) 11.3–11.73 (McGraw-Hill, 1993).
30. Gustafsson, J. P. Visual Minteq v. 2.50, revision 31/5/2006. Kungliga Tekniska Högskolan (2006); available at <http://www.lwr.kth.se/English/OurSoftware/vminteq/index.htm>.

Acknowledgements

This research was supported by the US National Science Foundation Life in Extreme Environments and Microbial Observatories programs; the National Oceanographic and Atmospheric Administration National Undersea Research Program; the Department of Energy; the American Chemical Society Petroleum Research Fund; the Environmental Protection Agency; the NASA Astrobiology Institute; and the Deutsche Forschungsgemeinschaft. We thank members of the LExEn 2002 shipboard scientific party and the ship and submersible crews from Harbor Branch Oceanographic Institution for help collecting and processing samples; Mitch Sogin and the Bay Paul Center at the Marine Biological Laboratory for efficient sequencing support; Basil Blake for painting Fig. 1; and A. Boetius, N. Finke and B. Gilhooly for providing comments that improved this manuscript.

Author contributions

S.B.J., V.A.S., I.R.M. and J.P.M. conceived the experiment and carried it out; K.-U.H. and M.E. completed the carbon isotopic analyses; A.P.T., K.G.L., M.A.L. and B.N.O. completed the molecular biological analyses; C.D.M. completed the thermodynamic calculations; S.B.J. wrote the paper and all authors provided editorial comments.

Additional information

Supplementary information accompanies this paper on www.nature.com/naturegeoscience. Reprints and permissions information is available online at http://npg.nature.com/reprintsandpermissions. Correspondence and requests for materials should be addressed to S.B.J.